

# Design of a Wide Tuning-Range, High Swing Fully Differential CMOS VCO with a Differential Tunable Active Inductor

Zahra Dorost Ghol<sup>1</sup>, Noushin Ghaderi<sup>2</sup>, Majid Ebnali-Heidari

1- Department of Engineering, Shahrekord University, Shahrekord, Iran  
Email: z.dorostghol@gmail.com (Corresponding author)

2- Department of Engineering, Shahrekord University, Shahrekord, Iran  
Email: ghaderi.nooshin@eng.sku.ac.ir

3- Department of Engineering, Shahrekord University, Shahrekord, Iran  
Email: ma.ebnali@gmail.com

Received: Dec. 2014

Revised: March 2015

Accepted: May 2015

## ABSTRACT:

In this paper, an inductor-less, high frequency tuning range and low power CMOS voltage controlled oscillator (VCO) is presented. The VCO can be implemented in 0.18  $\mu\text{m}$  CMOS, with 1.8 V supply voltage. By using a novel structure, a high frequency tuning range, low phase noise and low power consumption VCO, is obtained. In order to increase the frequency tuning range, an active inductor is used. In addition, deep triode region transistors are employed to enhance the swing of the output voltage. By using the results of simulation with HSPICE software, the tuning range, phase noise and power consumption are 5.49-9.6 GHz, -146 dBc/Hz and 5.99 mW, respectively.

**KEYWORDS:** CMOS ring oscillator, voltage controlled oscillator, tuning range, active inductor.

## 1. INTRODUCTION

Adjustable oscillators, which their output frequency is controlled by a voltage, are needed in many applications such as active Radio Frequency Identification (RFID) transponders, OC-48 application, frequency synthesizer module and PLL [1]. In addition, the oscillator with high frequency tuning range is desirable in modern communication systems. Generally, the CMOS oscillators are implemented at two types of ring oscillator and LC oscillator. In fact, the LC oscillators have low phase noise, better frequency stability and low power consumption compared to the ring oscillators. However, the LC oscillators will occupy a lot of places in circuit. In addition, frequency tuning range of LC oscillators is limited [2]. In high symbol rate of Gbps serial links, the slope of the rising and falling edges of the clock should be maximized to achieve the minimum timing jitter. The timing jitter of VCOs is obtained by Eq. 1 [3]-[4].

$$\overline{\Delta\tau^2} = \frac{v_n^2}{\left(\frac{dV}{dt}\right)^2} \quad (1)$$

Where the timing jitter, the threshold-crossings noise injected, and the threshold-crossings slew rate of the signal, are  $\Delta\tau^2$ ,  $v_n^2$  and  $\frac{dV}{dt}$  respectively. As shown in

Equation 1, the enhancement in the threshold-crossings slew-rate will decrease the timing jitter. The delay is developed by  $RC$  time constant at the fundamental nodes. This limitation is a conventional drawback of VCO structures [5]. In order to considerably improve the slew rate of the output voltage, the spiral inductors are employed at fundamental nodes. However, several limitations exist in utilizing spiral inductors as a load, including a large component size, large area and a small inductance. The active inductor in replace of spiral inductor is used to remove these limitations. Therefore by using a differential active inductor, a very wide frequency tuning range is obtained [6]. The ring oscillators with differential delay stage show the greater immunity to the common mode noise. Also, low phase noise and low power dissipation must be considered to the integration of oscillators [7]. In this paper, the design and calculations of a new active inductor VCO are provided. In section (2), the circuit design is described. In section (3), simulation results and discussions are presented. Conclusions are expressed in section (4).

## 2. DESIGN OF PROPOSED RING VOLTAGE OSCILLATOR

A ring oscillator is formed by a number of gain stages in a loop. Generally, its oscillation frequency changes

by using a controllable voltage. In fact, the output frequency of an ideal VCO has a linear relation with its control voltage. The oscillation frequency of an N-stage ring oscillator is  $2NT_d^{-1}$ , where  $T_d$  refer to the delay of each stage [1]. By considering the resistance load of the differential delay stage at the output node as  $R_{eq}$ , the time constant will be equal to  $R_{eq}C_L$  at the output node. Where,  $C_L$  is the capacitance of the differential delay stage at the output node [2]. Therefore, the oscillation frequency is equal to:

$$F_{osc} = \frac{1}{2NR_{eq}C_L} \quad (2)$$

The oscillation frequency, power, area and noise performance are the key roles of the ring VCO design [2]. Indeed, superior frequency tuning range, low power, low area and low noise performance are desirable. In this paper, a two-stage ring oscillator VCO is proposed. Its structure is shown in Figure 1. The circuit of each delay stage is illustrated in Figure 2 [8]. Each delay stage circuit (Figure 2) has two poles and one zero. The value of zero, neutralizes the small pole. Therefore the second pole that located at higher frequencies, remains and causes to increase the bandwidth. The active inductor is employed in this circuit to avoid a large chip area. In this circuit,  $M_1$  and  $M_2$ , are used as input pair. In addition, an active inductor as is shown in Figure 3, is provided to increase the frequency range [9].

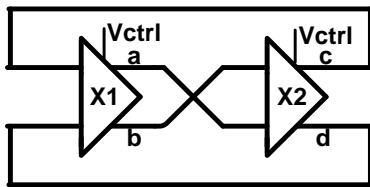


Fig. 1. Architecture of the two-stage ring oscillator

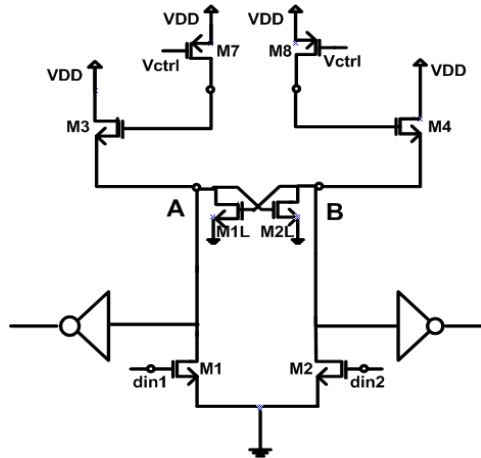


Fig. 2. delay stage for ring oscillator [8]

The equivalent resistance of the active inductor circuit is obtained as follows [9]-[10];

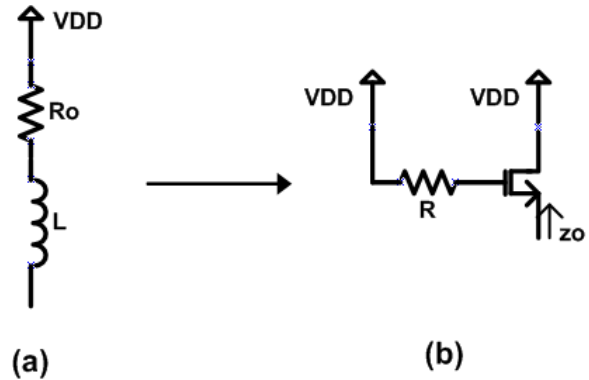


Fig. 3. Active inductor load [9]-[10]

$$Z_o = \frac{S(C_{gd} + C_{gs}) + \frac{1}{R}}{S^2 C_{gd} \cdot C_{gs} + S(\frac{C_{gs}}{R} + C_{gd} \cdot g_m) + \frac{g_m}{R}} \cong \frac{1}{g_m} + S \frac{RC_{gs}}{g_m} \quad (3)$$

By using the spiral inductor as a load, as it is shown in Figure 3(a), the transfer function of the delay stage is obtained by Equations 4 and 5:

$$A_v(j\omega) = -g_{m1} \left[ \frac{-1}{g_{m1L}} \parallel \frac{1}{j\omega C} \parallel (R_o + j\omega L) \right] \quad (4)$$

$$A_v = \frac{-g_{m1}(R_o + j\omega L)}{(1 - R_o g_{m1L} - \omega^2 LC) + j\omega (R_o C - g_{m1L})} \quad (5)$$

Where, C is the parasitic capacitance at the output node.

According to Barkhausen's criteria, at oscillation frequency of a ring oscillator, the total phase shift of a delay stage chain must be  $180^\circ$  in feedback system. Therefore, in a two stage ring oscillator, the phase shift of the transfer function will be equaled to  $90^\circ$ .

It means that, the oscillation frequency will be obtained as follows:

$$F_{osc} = \frac{1}{2\pi} \sqrt{\frac{R_o(1 - R_o g_{m1L})}{L \cdot g_{m1L}}} \quad (6)$$

Therefore, if L is decreased,  $F_{osc}$  will be increased. According to Equation 3,  $R_o$  is equaled to  $1/g_{m3,4}$ . The size of  $M_{1L,2L}$  and  $M_{3,4}$  is chosen to have the value of  $R_o g_{m1L,2L}$  lower than one.

As can be seen in Figure 2, the loads of delay stage are consisted of controllable transistors  $M_7$  and  $M_8$ . By using a variable load through varying the gate voltage of  $M_7$  and  $M_8$ , the oscillation frequency can be tuned. If  $M_7$  and  $M_8$  transistors are biased in deep triode region, the resistance values of  $M_7$  and  $M_8$ , are obtained as follows:

$$R_{M7,8} = \frac{1}{\mu_p C_{ox} (\frac{W}{L})_{7,8} (V_{DD} - V_{ctrl} - |V_{thp}|)} \quad (7)$$

According to the above equation, by decreasing  $V_{ctrl}$ ,  $R_{M7,8}$  will be decreased. It means that, the inductance will be decreased according to the following relation:

$$L = \frac{R_{M7,8} C_{gs3,4}}{g_{m3,4}} \quad (8)$$

Therefore, according to Equation 6, the oscillation frequency will be increased.

By using crossover transistor pair,  $M_{1L}$  and  $M_{2L}$ ,  $90^\circ$  delay will be obtained by each delay cell. It means that, the Barkhausen's criteria will be satisfied by this oscillator. In addition, these transistors are used to charge and discharge of output node capacitor faster. The action of the delay stage can be characterized as follows:

1. If the input node of din1 becomes lower than another input node of din2, then  $M_2$  will be on, while  $M_1$  will be off. Consequently,  $M_{2L}$  will be on and  $M_{1L}$  will be off. It means that, the output node (B) capacitor will be discharged through  $M_{2L}$  transistor.
2. If the input node of din1 becomes larger than another input node of din2, then  $M_1$  will be on, while  $M_2$  will be off. Consequently,  $M_{1L}$  will be on and  $M_{2L}$  will be off. Therefore, the capacitance at the output node (B) doesn't discharge through  $M_{2L}$  transistor. This capacitor will be charged through  $M_4$  and controllable  $M_{7,8}$  transistor (near  $V_{DD}$ ). In both actions of the full circuit, controllable PMOS transistors of  $M_7$  and  $M_8$ , adjust the entire charging and discharging of capacitors at the output node of delay stage.

One of the most important problems of this circuit (Figure 2) is its limited frequency tuning range. Another problem of the circuit is its limited output voltage swing, which is caused by using the active inductor. Triode region transistors  $M_5$ ,  $M_6$ ,  $M_{77}$  and  $M_{88}$  are added to solve the above problems, which are shown in Figure 4.

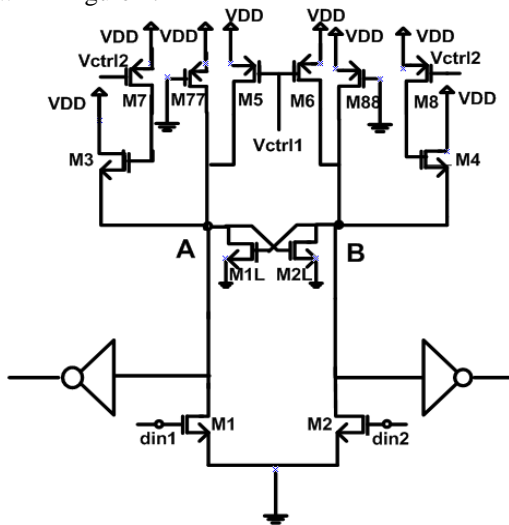


Fig. 4. Frequency range of the proposed ring oscillator

The dc equivalent resistance at the output node is given by Equation 9. It shows that  $R_{eq}$  has a small value, which cause to improve the oscillation frequency and frequency tuning range.

$$R_{eq} = \left( \frac{1}{g_{m3,4}} \parallel \frac{-1}{g_{m1L,2L}} \parallel R_L \right) = \frac{1}{g_{m3,4} - g_{m1L,2L} + \frac{1}{R_L}} \quad (9)$$

The value of  $R_L$  in Equation 9 is obtained as follow;

$$R_L = R_{M5,6} \parallel R_{M77,88} \quad (10)$$

$R_{M5,6}$  are biased in deep triode region. Therefore they have a small output resistance. As mentioned before, if the value of  $V_{ctrl}$  becomes low,  $R_{M5,6}$  and therefore  $R_L$  will be decreased, while the values of  $g_{m3,4}$  and  $g_{m1L,2L}$  are constant. According to Eq. 9, if  $R_L$  is decreased,  $R_{eq}$  will be decreased. It means that, the oscillation frequency will be increased. Indeed, according to the Equation 2, conclusion can be obtained as follows:

$$V_{ctrl} \downarrow \rightarrow R_L \downarrow \rightarrow R_{eq} \downarrow \rightarrow F_{osc} \uparrow \quad (11)$$

### 3. SIMULATION RESULTS

The proposed voltage controlled ring oscillator circuit is simulated based on TSMC 0.18 $\mu$ m CMOS process model using HSPICE. The tuning range of Figure 2 and proposed VCO are shown in Figure 5 and Figure 6, respectively, where  $V_{ctrl1}$  and  $V_{ctrl2}$  are connected together and considered as a single  $V_{ctrl}$  in the proposed VCO. As can be seen, the frequency tuning range is higher in the proposed VCO. Furthermore, the performance of its linearity is much better. In the proposed VCO circuit, the control voltage value is varied between 0 to 1.3V, which cause in a frequency range of 9.6 GHz to 5.49 GHz (Figure 6). Otherwise, if  $V_{ctrl1}$  is changed between 0 to 1.3V and  $V_{ctrl2}$  is fixed at 0V, the frequency tuning range will be changed between 9.6 GHz to 8.43 GHz, as is shown in Figure 7. Also, if  $V_{ctrl2}$  is changed between 0 to 1.3V and  $V_{ctrl1}$  is fixed at 0V, the frequency tuning range will be changed between 9.6 to 7.36 GHz (Figure 8). As can be seen, by integrating the Figures 7 and 8 together, Figure 6 will be obtained, which is a more linear function of  $V_{ctrl}$ . The differential waveforms of the VCO at a frequency of 7.64 GHz are illustrated in Figure 9. The output spectrum which is simulated at 7.64 GHz is shown in Figure 10. The simulation result illustrates a maximum peak at 7.64 GHz of oscillation frequency, with the spectrum of complementary skirting spurs. Eye diagram and jitter histogram at 7.64 GHz working frequency are illustrated in Figures 11 and 12. These figures exhibit about 2.58ps and 3.3 ps RMS and peak-to-peak jitters, respectively. By using Equation 12, the phase noise is obtained as follows [3]:

$$S_\phi = \frac{f_0}{f^2} \times \left( \frac{\Delta f_{vco-ms}}{T_0} \right)^2 \quad (12)$$

Where,  $f_0$  is center frequency,  $f$  is certain frequency offset,  $\Delta t_{vco-rms}$  is rms jitter, and  $T_0$  is period of signal. The phase noise of the VCO at the working frequency in different frequency offset is presented in Figure 13. The output phase noise is -146 dBc/Hz at a 1MHz frequency offset. The value of merit of the proposed VCO according to Equatin 13 [11], is -208 dBc/Hz.

$$FOM = L\{\Delta f\} - 20\log\left\{\frac{f_0}{\Delta f}\right\} + 10\log\left\{\frac{P_{diss}}{1mW}\right\} \quad (13)$$

Where,  $L\{\Delta f\}$ ,  $\Delta f$ ,  $f_0$  and  $P_{diss}$  are phase noise, certain frequency offset, center frequency and power dissipation, respectively. A comparison between proposed work with previous ring oscillators is performed in Table 1. The proposed oscillator obtained a FOM of -208 dBc/Hz. In the proposed ring oscillator the frequency tuning range is increased and the value of phase noise is almost improved while the power consumption of the ring oscillator is minimum.

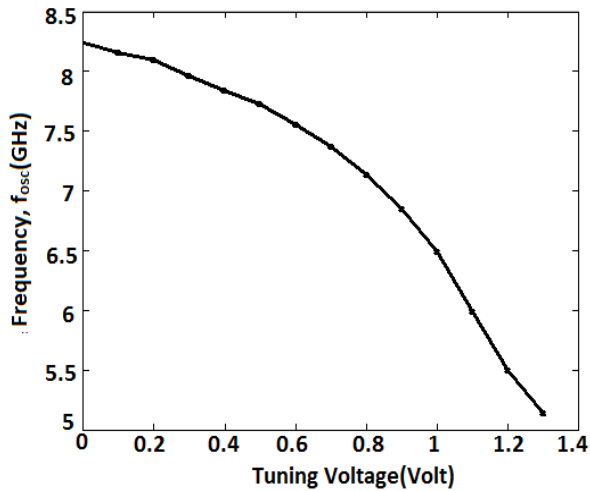


Fig. 5. Frequency range of the Fig. 2

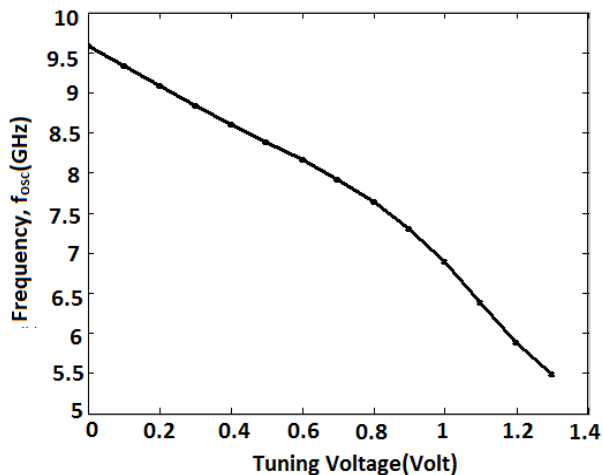


Fig. 6. Frequency range of the proposed ring oscillator

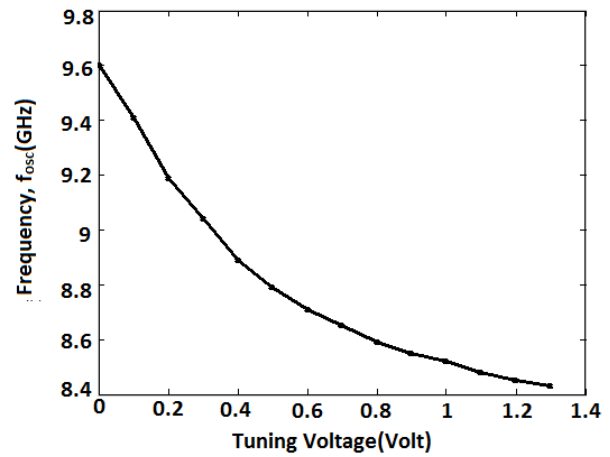


Fig. 7. Frequency range of the proposed ring oscillator for Vctrl1 variations and constant Vctrl2

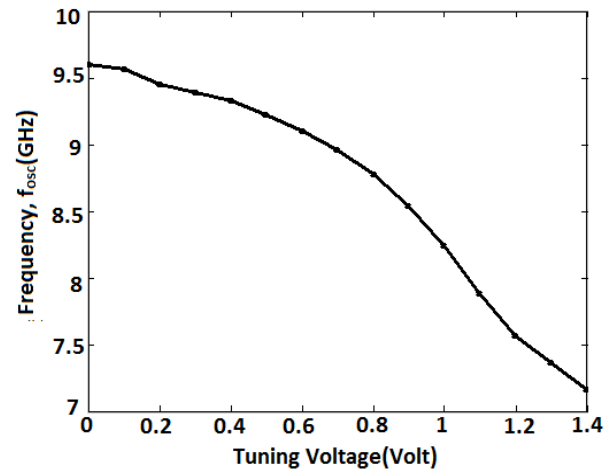


Fig. 8. Frequency range of the proposed ring oscillator for Vctrl2 variations and constant Vctrl1

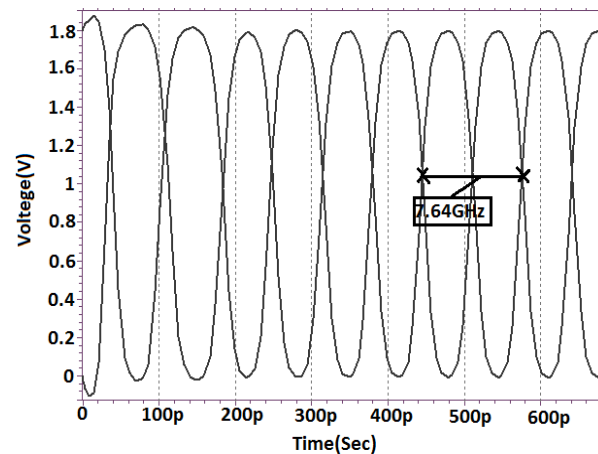


Fig. 9. Transient response of VCO at 7.64 GHz

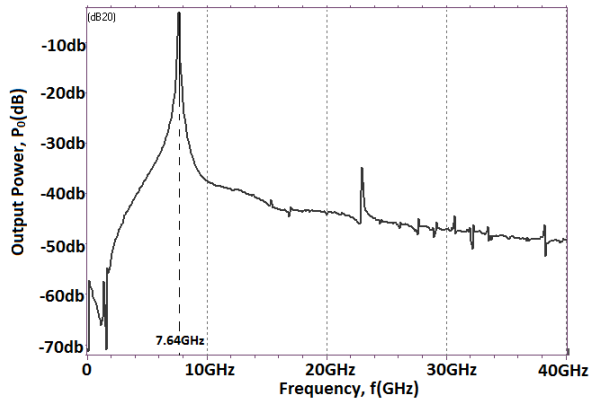


Fig. 10. Output spectrum of the VCO at center frequency

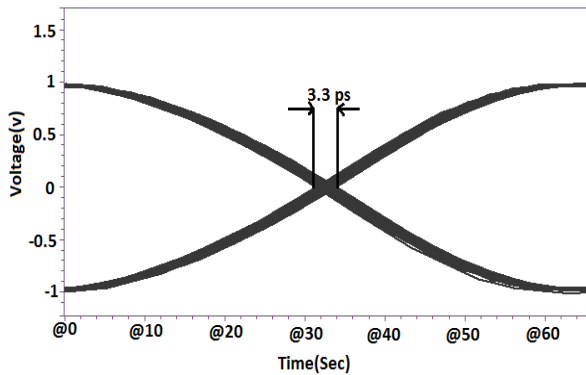


Fig. 11. Output jitter eye diagram at 7.64 GHz

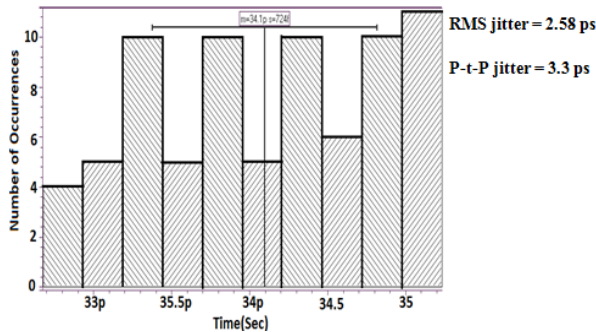


Table 1. The performance comparisons of ring oscillators

Ring Oscillator	CenterF req (GHz)	Tuning Range (GHz)	Phase Noise (dbc/Hz)	SupplyV oltage (V)	FOM (dbc/Hz)	Power (mW)	Technology ( $\mu$ m)	No. of stages
Proposed	7.64	5.49-9.6	-146@1MHz	1.8	-208	5.99	0.18	2
[2]	0.9225	0.92-0.925	-116@10MHz	3.3	-138.97	42.9	0.35	3
[7]	2.4	1.6-2.6	-141@1MHz	1.8	-208	1.09	0.18	3
[12]	2.45	2.36-2.85	-112@10MHz	1.8	-151.34	6.99	0.18	3
[15]	-	1.72-1.92	-123.4@10MHz	1.8	-	13	0.18	4
[16]	0.886	0.381-1.15	-126@10MHz	3.3	-156	7.48	0.35	3
[17]	-	1.57-3.57	-90.31@0.6MHz	1.8	-	16.8	0.09	2
[18]	1.35	0.62-1.5	-126@1MHz	1.8	-172.5	41	0.18	4

Fig. 12. Output jitter histogram at 7.64 GHz

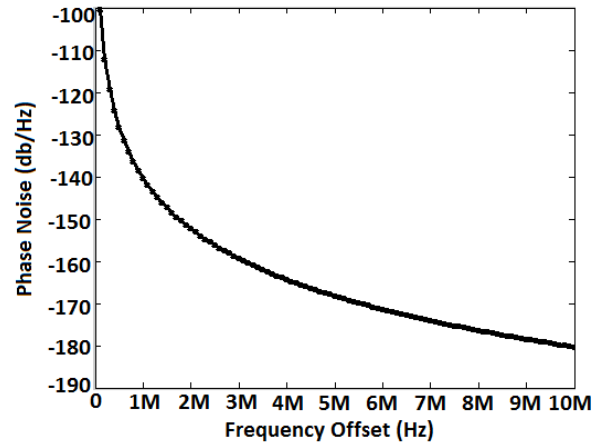


Fig. 13. Simulated phase noise at 7.64 GHz for different frequency offsets

#### 4. CONCLUSIONS

In this paper, a two-stage differential ring oscillator is presented. By using an active inductor in each delay stage, a wide tuning range is obtained. In addition, the deep triode region transistors are used to increase the swing of the output voltage. The results show that maximum tuning range, phase noise and power consumption are 5.49-9.6 GHz, -146 dBc/Hz and 5.99 mW, respectively. This circuit illustrates a high FOM performance compared to the previous works. Thus this VCO can be expressed as one of the high tuning range VCO, which is suitable for PLL applications.

## REFERENCES

- [1] B. Razavi, "Design of analog CMOS integrated circuits", Ed. New York, NY, USA: McGraw-Hill, 2001.
- [2] S. Ling, T. Lu, J. Wei-ping, X. Jun, "CMOS ring VCO for UHF RFID readers", *Science Direct J. China Universities of Posts and Telecommunications*, pp. 20-23, June 2010.
- [3] T. Ch. Weigandt, "Low-Phase-Noise, Low-Timing-Jitter Design Techniques for Delay Cell Based VCOs and Frequency Synthesizers", *PhD dissertation*, Univ. California, Berkeley, 1998.
- [4] T. Weigandt, B. Kim and P. Grey, "Analysis of timing jitter in ring oscillators", *In Proc. 1994 IEEE Int'l Symposium of Circuits Systems*, pp. 27-30.
- [5] M. El-Hage and F. Yuan, "Timing jitter analysis of delay cells of CMOS voltage controlled oscillators", *In IEEE Canadian Conf. on Elec. and Comp. Engineering, Niagara Falls, Ontario, Canada*, vol. 3, pp. 1785-1788, 2004.
- [6] L. H. Lu, H. H. Hsieh, and Y. T. Liao, "A Wide Tuning-Range CMOS VCO With a Differential Tunable Active Inductor", *IEEE Trans. on Microwave Theory and Techniques*, Vol. 54, No. 9, pp. 3462-3468, September 2006.
- [7] H. Ramiah, Ch. W. Keat, and J. Kanesan, "Design of Low-phase Noise, Low power Ring Oscillator for OC-48 Application", *IETE J. Research*, Vol. 58 Issue 5, pp. 425-428, 2012.
- [8] E. Sackinger, W. Fischer, "A 3-GHz 32-dB CMOS limiting amplifier for SONET OC-48 receivers", *IEEE J. Solid-State Circuits*, Vol. 35, pp. 1884-1888, 2000.
- [9] K. Gupta, N. Pandey, and M. Gupta, "A New Active Shunt-Peaked MCML Based High Performance 1:8 Demultiplexer For Serial Communication", *Int. J. Engineering Science and Technology*, Vol. 2(9), pp. 4632-4639, 2010.
- [10] F. Yuan, "CMOS Active Inductors and Transformers", *Springer*, Ed. Toronto, Ontario, Canada, pp. 21-98, 2008.
- [11] J. Kim, J. O. Plouchart, N. Zamdmmer, R. Trzcinski, K. Wu, B. Jeffrey Gross, and M. Kim, "A 44GHz Differentially Tuned VCO with 4GHz Tuning Range in 0.12  $\mu\text{m}$  SOI CMOS", *Int. J. Engineering Science and Technology*, Vol. 2(9), pp. 4632-4639, 2010.
- [12] J. Jalil, M. B. I. Reza, M. A. M. Ali, and T. G. Chang, "A Low Power 3-Stage Voltage-Controlled Ring Oscillator in 0.18  $\mu\text{m}$  CMOS Process for Active RFID Transponder", *J. Elektronika IR Elektrotehnika*, ISSN 1392-1215, Vol. 19, No. 8, 2013.
- [13] W. H. Tu, J. Y. Yeh, H. Ch. Tsai, and Ch. K. Wang, "A 1.8V 2.5-5.2 GHz CMOS Dual-input Two-stage Ring VCO", *IEEE Asia-Pacific Conf. on Advanced System Integrated Circuits*, pp. 134-137, 2004.
- [14] S. Zheng, L. He, "The Mixed-Signal Design of PLL with CMOS Technology", *Int'l Symposium of Signals, Systems and Electronics (ISSSE)*, 2007.
- [15] Z. Z. Chen, T. Ch. Lee, "The Design and Analysis of Dual-Delay-Path Ring Oscillators", *IEEE Trans. on circuits and systems I: Regular Papers*, Vol. 58, No. 3, pp. 470-478, 2011.
- [16] H. Thabet, S. Meillere, M. Masmoudi, J. L. Seguin, H. Barthelemy, and Kh. Aguir, "A Low Power Consumption CMOS Differential-Ring VCO for a Wireless Sensor", *IEEE 9th Int. Conf. New Circuits and Systems (NEWCAS)*, pp. 81-84, 2011.
- [17] J. K. Panigrahi, D. P. Acharya, "Performance Analysis and Design of Wideband CMOS Voltage Controlled Ring Oscillator", *IEEE 5th Int. Conf. on Industrial and Information Systems, ICIIS*, pp. 234-238, 2010.
- [18] S. U. Lee, Sh. Amakawa, N. Ishihara, and K. Masu, "Low-Phase-Noise Wide-Frequency-Range Differential Ring-VCO with Non-Integral Subharmonic Locking in 0.18  $\mu\text{m}$  CMOS", *40th Conf. European Microwave*, pp. 1611-1614, 2010.
- [19] F. Kh, T. A. Ch, "Design of Ring VCO using NINE Stages of Differential Amplifier", *Int. J. Research in Engineering and Technology*, Vol. 3, pp- 2321-7308, 2014.
- [20] F. Yuan, "A Fully Differential VCO Cell with Active Inductors for Gbps Serial Links", *Springer Science J. Analog Integrated Circuits and Signal Processing*, Vol. 47, pp. 213-223, 2006.
- [21] S. M. Chueng, "The Study of CMOS Based VCO with Active Inductor and ITS Design Methodology", Master of Science, Graduate School-New Brunswick Rutgers, The State Univ. New Jersey, 2012.